Eur. Phys. J. Plus (2025) 140:307
https://doi.org/10.1140/epjp/s13360-025-06199-y

THE EUROPEAN PHYSICAL JOURNAL PLUS

Regular Article

Design and experimental validation of a compact spectrometer for epithermal neutrons

E. Mafucci[1,2,a], **V. Monti**[1,2], **V. Barletta**[1], **M. Costa**[1,2], **E. Durisi**[1,2], **M. Marchisio Caprioglio**[1], **M. Riberti**[1], **R. Bedogni**[3]

[1] Università degli studi di Torino, Via P. Giuria 1, 10125 Turin, TO, Italy
[2] INFN, Sezione di Torino, Via P. Giuria 1, 10125 Torino, TO, Italy
[3] INFN, Frascati National Laboratories, Frascati, Italy

Received: 3 February 2025 / Accepted: 7 March 2025

Abstract A novel neutron compact spectrometer with an isotropic response called Neutron Capture Therapy Activation Compact Spectrometer is presented (**). The device is sensitive from thermal up to 100 keV neutrons, and it is designed for working in a single irradiation exposure. The detector geometry is composed by a spherical moderator shell containing different material foils exhibiting neutron radiative capture resonances covering the epithermal energy domain. The simulation results on the geometry optimization and on the elements choice will be presented. Irradiation and activation measurements on a first prototype have been performed at a calibrated epithermal neutron source in Torino. The unfolded neutron spectrum was compared with those obtained using a Bonner Sphere Spectrometer, showing an agreement within few %. This serves as a proof of concept. ACS is a promising device for neutron applications, such as Boron Neutron Capture Therapy, where an epithermal neutron beam or field is involved. Due to the compact dimensions, it could also be utilized for in-phantom measurements.

1 Introduction

In recent years, the introduction of accelerator-based Boron Neutron Capture Therapy (BNCT) facilities has led to a significant increase in interest from the medical and scientific communities. Monitoring and characterization of neutron beams and inter-comparison of different facilities are becoming mandatory [1]. This stimulates the development of dedicated dosimetry and spectrometry techniques. The neutron energy for the BNCT application ranges from thermal up to 100 keV, covering the whole epithermal domain. The standard technique for measuring the neutron spectra consists in the use of a Bonner Sphere Spectrometer (BSS) [2]. This technique works by placing a thermal neutron detector at the center of polyethylene spheres of different diameters. These spheres act as moderators, slowing down fast neutrons to thermal energies. The larger the sphere, the more effective it is at moderating neutrons. As each sphere exhibits a different energy-dependent response, spectrometric information can be obtained by studying the variation of the counting rate as a function of the sphere diameter. Then, the spectrum can be reconstructed via an unfolding procedure. This method allows for the characterization of neutron fields in complex environments. Nevertheless, this technique presents some difficulties in measuring the neutron spectra under such particular conditions, as in the case of the BNCT. The BSS requires large spaces to work: typically around 20 - 30 cm for measuring low energy neutron up to 1 MeV, but even larger spaces for a complete BSS device capable of measuring also the high energy neutron component. Such dimensions are not compatible for in-phantom measurements in which the detector size should be less than 15 cm. Furthermore, the response of a BSS along the epithermal energy range lacks in terms of energy resolution [3], producing high uncertainties and low sensibility to changes in the spectrum shape. Finally, the exposure of many different spheres leads to a long measurement which can hardly match the need to carry out daily routine measurements. A possibility to overcome the BSS limitations is to take advantage of other neutron detection mechanisms instead of solely the thermal capture reaction. In particular, the epithermal neutron capture process can be a valid alternative, since for some elements it presents high and well-known cross-section values. Moreover, because the neutron capture occurs in the epithermal energy domain, the moderator thickness can be reduced. This allows scaling down the overall dimensions. The goal of this work is to develop a spectrometer that could work in the epithermal energy range, with a high energy resolution and with measurement operations in a single exposure operation. Such device may be considered as a novelty in the neutron spectrometry field.

[a] e-mail: ettoremarcello.mafucci@unito.it (corresponding author)

Published online: 15 April 2025

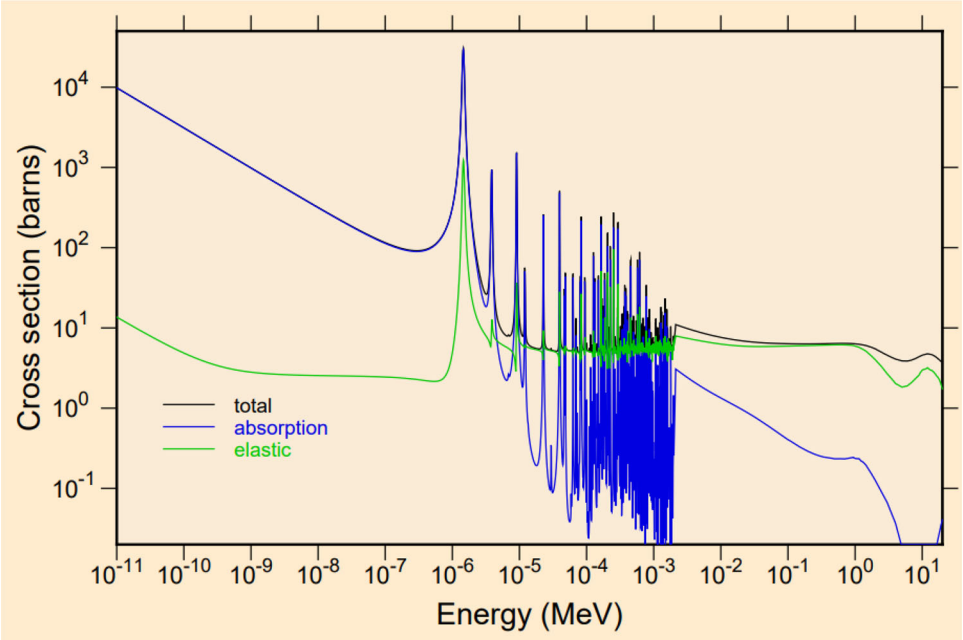

Fig. 1 ^{115}In neutron cross sections, data are taken from [4]. A strong capture resonance, dominating among the others, is visible at around 1.5 eV

2 The ACS concept

The **A**ctivation **C**ompact **S**pectrometer (**ACS**) is a neutron spectrometer based on the activation phenomenon, characterized by dimensions in the order of few centimeters. The primary concept behind ACS involves using the characteristics of neutron cross sections within the epithermal range. Each element possesses a distinct neutron capture cross section due to the different nuclear structure. Some elements exhibit a pronounced resonance in their cross section which dominates over the other resonances (e.g. Fig. 1).

After a careful selection of elements with the main resonance positioned at different energies, the whole epithermal range can be sampled (Sect. 2.1).

The activation values of the different elements can be measured via a calibrated gamma detector. A relationship between the induced activities and the number of capture reaction can be determined (Sect. 3).

In order to reconstruct the neutron spectrum, advanced analytical techniques are required (Sect. 4).

An exhaustive description of the whole process can be found in [5], while a shorter summary can be found in [6].

The main ACS properties are:

1. **Energetic sensitivity: from thermal up to 100 keV.** This energy range covers the whole epithermal domain in which most of the neutron resonances are located.
2. **Dimensions: few cm.** The small size allows performing measurements in reduced spaces, overcoming the problems related to the BSS dimensions.
3. **Angular response: isotropic.** An isotropic response is essential to ensure that the detector is not influenced by the angular distribution of the neutron source. In many cases, this distribution is not well known, and the surrounding environment can also alter it. A detector that does not exhibit an isotropic response would yield different measurements depending on its position and orientation relative to the source. This could introduce significant systematic uncertainties. Thus, an isotropic response is highly recommended for spectral neutron measurements (like in the BSS case).
4. **Working conditions: single exposure.** This feature reduces the overall measuring time, making the spectrometer suitable for daily routine measurements.
5. **Machinability: easy to be constructed and used in all the situations.** A complex geometry brings difficulties in the realization and in the measurements.

The ACS study was divided into two main areas: the elements selection and the geometry optimization. Both have an impact on the final characteristics, but can be analyzed separately, finding the right compromise.

Table 1 Selected elements with their main characteristics

Element	Isotopic %	E_r (eV)	$t_{1/2}$	E_γ (keV)	I (b)
^{115}In	95.70	1.56	54.41 min	1293.5	2638
^{185}Re	37.40	3.4	3.718 d	137.2	1632
^{197}Au	100	5.65	2.695 d	411.8	1550
^{186}W	28.43	20.5	23.72 h	479.6	550
^{187}Re	62.60	41.1	17.01 h	155	318
^{55}Mn	100	468	2.579 h	846.8	13.9
^{63}Cu	69.17	1040	12.7 h	511	4.88
^{23}Na	100	3380	14.96 h	1368.6	0.303
^{51}V	99.75	7230	3.75 min	1434.1	2.63

From left to right: isotopic abundance, main resonance energy, half-life time, energy of the emitted gamma and resonance integral value

2.1 Elements selection criteria

All the nuclear data used have been obtained from [4, 7–10]. Many beta decay data have been taken from the Table of Radioactive Isotopes Database [11], almost all data shown in this database are from the evaluated nuclear structure file (ENSDF). ENSDF is updated and maintained by the National Nuclear Data Center (NNDC) at BNL. Reference to [12] has been also useful for its valuable work.

To select the best candidates, many criteria were chosen, taking into account physical, practical, economic, and safety aspects:

- The general request was to use solid elements with high isotopic abundance and no natural toxicity nor radioactivity.
- The elements were selected in such a way their resonances were well distributed overall the epithermal energy range. The effective resonance energy [13] can be calculated using equation 1:

$$ln(\bar{E}_r) = \frac{\sum_i w_i \, ln(E_{r,i})}{\sum_i w_i} \tag{1}$$

Being $E_{r,i}$ the different resonances energy and w_i the weighting factors, given by:

$$w_i = \left(\frac{g\Gamma_\gamma \Gamma_n}{\Gamma}\right)_i \frac{1}{E_{r,i}^2} \tag{2}$$

Where g, Γ_γ, Γ_n, $\Gamma = \Gamma_\gamma + \Gamma_n$ are respectively the nuclear spin factor, the capture width, the interaction width, and the total width. This selection allowed to have enough energy sensitivity and to avoid the lack of resonances in certain energy region. An effort was made to have at least two elements per order of magnitude in the effective resonance energy distribution (0 - 10 eV, 10 - 100 eV, 100 - 1000 eV, 1 - 10 keV, 10 - 100 keV). Moreover, if more elements were sensitive to the same energy range, the two with the higher resonance integral value were preferred [14], where the resonance integral I is defined in equation 3:

$$I = \int_{0.4\,eV}^{+\infty} \frac{\sigma(E)}{E} dE \tag{3}$$

All the data for this selection have been taken from [8]. The absolute value for the activation induced during the neutron irradiation strongly depends by I:

$$A_r = N\dot{\phi}_{epi} I \tag{4}$$

Being $\dot{\phi}_{epi}$ the epithermal fluence rate and N the number of target nuclei.

- The activated candidates should present adequate decay scheme and modality. The half-life time should range from few minutes (> 3 min) up to few days (< 4 d). For daily routine measurements, a long half-life time element would represent a limit. More than a single unit can be purchased and used in rotation, but this aspect should be limited to not increase the cost. High (> 2 MeV) and low (< 20 keV) energy gamma should be avoided due to efficiency detection and γ natural background. Moreover, the higher branching ratios were preferred to achieve higher statistics. Finally, elements with a simple decay scheme were preferred. Thus, elements with a high number of γ emitted or elements with multiple in-chain decay were considered less attractive.
- Good machinability and low commercial price were preferred. These criteria were applied only in the final step and were introduced with the aim of developing a more marketable product.

The final selected elements with their main characteristics are listed in Table 1.

From Table 1, it can be seen that the effective resonance energies cover the epithermal range up to the order of magnitude of 1 - 10 keV. No good candidates were found for the highest energy domain (10 - 100 keV). To overcome this issue and to extend the ACS sensitivity, the use of a moderator has been considered. Moreover, the differences in the integral resonance values (last column) can be reduced considering different values in thickness for the different elements. A simulations study has been done and is presented in the following section (Fig. 2).

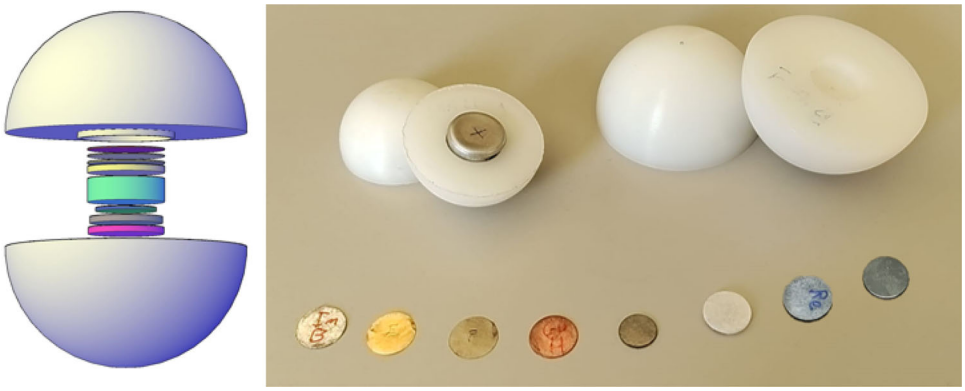

Fig. 2 Left: geometry scheme for the Monte Carlo simulation with a moderator sphere shell. Right: shot of the two built prototype with radius of 20 mm and 28 mm

2.2 Geometry validation

An extensive Monte Carlo study on the ACS geometry was performed using the MCNP6 code. The thicknesses of the different foils were tuned in order to partially compensate the different resonance integral values and are shown in Table 1. Similar induced activities for the selected elements would simplify the data acquisition. Moreover, from a preliminary Monte Carlo analysis, the resonance peaked structures were noted to introduce nonphysical fluctuations in the neutron spectrum reconstruction since the unfolding procedure was not able to properly work with such narrow response curves. The introduction of a small moderator shell was considered again as a possible solution. The scope of the moderator in ACS is therefore twofold: it smooths the response curves, enabling the unfolding procedure, and it also extends the energy sensitivity over 10 keV. An effort on the simulation work was made to find the best compromise between these aspects. Moreover, the isotropic response can be achieved considering simpler foils geometry (Fig. 3).

Combining all these information, the final ACS geometries are shown in Fig. 2 and are characterized by:

- **An outer HPDE spherical shell.** The external part is composed by a HDPE (high-density polyethylene) sphere with a radius that can range from 20 mm up to 30 mm. Values outside this range bring to issues in the isotropy of the system or in the unfolding procedure.
- **An inner cadmium hollow cylinder.** Inside the moderator sphere a Cd hollow cylinder is placed to suppress the thermal component and be sensitive only to the epithermal neutron component. The cylinder is 12 mm high, and the external radius is 7 mm with a thickness of 0.5 mm.
- **A sensitive part.** It is composed of 8 foils: In, Au, Re, W, Mn, Cu, NaCl, V; arranged together as listed. Monte Carlo simulations shown that the displacement order is not relevant, however, the same disposition has been used for all the measurements to improve the reproducibility. All the foils are placed inside the Cd cylinder. This configuration corresponds to 9 sensitive isotopes since ^{185}Re and ^{187}Re are both interesting for the ACS scope. The radius of the foils ranges from 5.0 mm to 6.3 mm (depending on the commercial availability) and the thickness from 51 μm to 3.8 mm.

3 The HPGe gamma detector calibration

The HPGe detector used for the activation analysis was an ORTEC gem20p4-70 [15]. The detector is fabricated from P-type germanium with an outer contact of diffused Li and an inner contact of ion-implanted boron. The sensor diameter is 2", the response time is in the order of 8-10 ns and the efficiency, relative to a 2.5" NaI(Tl) scintillator, is 20%. The energy resolution at 122 keV, 662 keV, and 1333 keV are respectively 0.67, 0.3, and 0.14%.

The detector has been calibrated through a two-steps process.

Efficiency Calibration:

The absolute efficiency was estimated placing calibration sources at 10 cm from the Al cup covering the sensitive region. The calibration sources used were: ^{133} Ba, ^{137} Cs, ^{22} Na, ^{60} Co, ^{152}Eu for a total of 18 energy calibration points. An interpolation fit to extract the functional form that best represented the efficiency as a function of energy was applied. The formula 5 proposed by Debertin et al. [16] (page 213-222) was employed assuming n=3:

$$log\,\epsilon = \sum_{j=0}^{n} p_j \left(log \frac{E}{E_0} \right)^j \qquad E_0 = 1keV \tag{5}$$

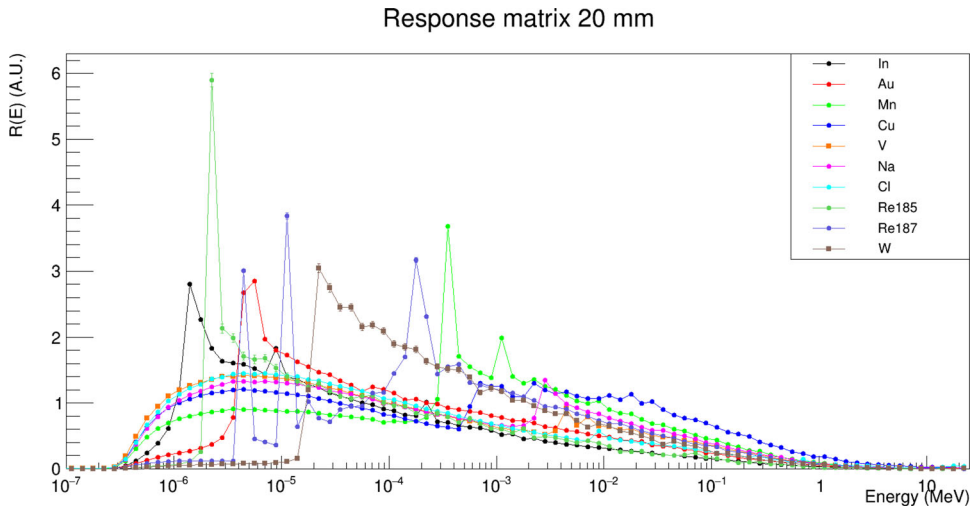

Fig. 3 Monte Carlo response matrix for the ACS 20 mm radius configuration. The data have been normalized to the unit area; the resonance integral values are listed in Table 1. The shape of the response functions reveals the presence of a peaked structure in correspondence with the capture resonance and a continuum due to the moderator. The anisotropy response was evaluated through Monte Carlo simulations as the dispersion of the induced activity values, varying the angle between the incoming neutron and the foil surfaces from 0° to 180° in 15° steps. In the simulations, the source was modeled as an ideal planar source, and the simulated neutrons were monodirectional at different angles within this range. In this configuration, the estimated dispersion was found to be below 2.5% ([5], pp. 100-110)

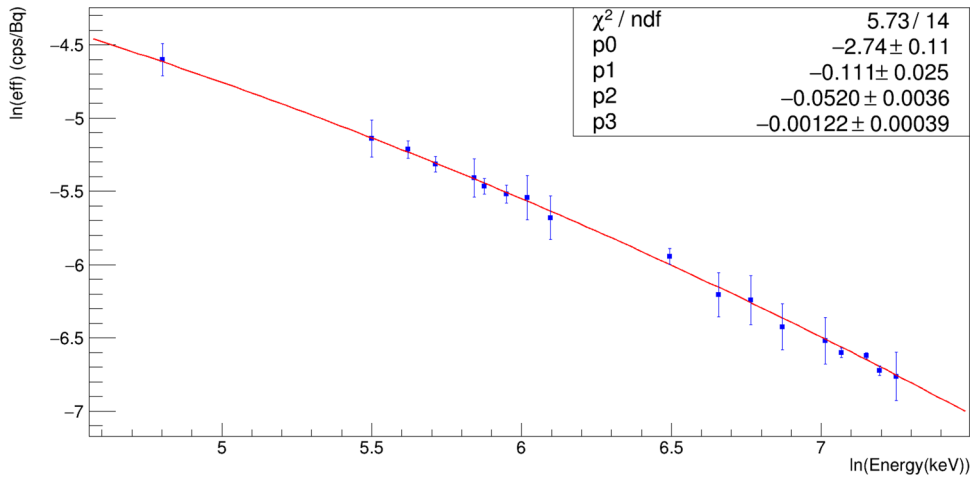

Fig. 4 In blue, the 18 measured points are shown; the sources were placed at 10 cm by the detector. In red, the fit model is shown

The result of the calibration with the fitting function is shown in Fig. 4. After this first step, the efficiency value for a point like source at a certain energy can be extracted considering the fit equation (see Fig. 4).

Geometric factor determination:

To evaluate the absolute activity of the foils, it is possible to perform a measure at a distance of 10 cm from the detector. In this condition, the point source like approximation is good enough. However, this measurement demands high activity levels or prolonged exposure times. A contact condition not only would facilitate the activities measure, but also would reduce the acquisition time being more interesting for the daily routine. Thus, for once, each foil composing the sensitive part of ACS was exposed to the Torino LINAC facility e-LiBANS [17] and the counts per second (cps) using the HPGe were registered at contact (cps_1) and at a distance of 10 cm (cps_2). By applying the correction in eq. 6, the loss of activity during the measurement is assessed:

$$k_c = \frac{A_0}{\bar{A}} = \frac{A_0}{1/t_c \int_0^{t_c} A(t)dt} = \frac{t_c}{\tau\left(1 - e^{-t_c/\tau}\right)} \tag{6}$$

The correction factor k_c, (where c means *counting*) is calculated making the ratio between the initial value of activity A_0 and the mean integral value of the well-known function activity time. Another correction is due to the delay time between the two measurements and it is presented in eq. 7:

$$k_d = e^{-\frac{t_d}{\tau}} \tag{7}$$

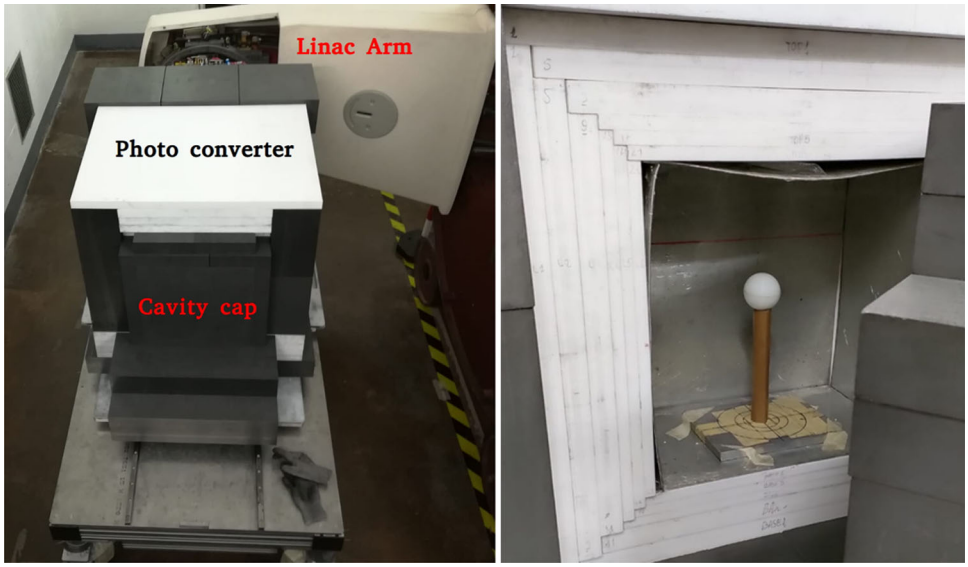

Fig. 5 Experimental setup for testing the ACS prototype. Left: the e-LiBANS facility in the epithermal configuration. Right: the ACS 20 mm radius configuration inside the cavity

Being t_d the delay time. Finally, the evaluation of the cps ratio can be performed, this value denotes the geometric scaling factor F_g between the induced counts in contact and at distance (Eq. 8).

$$F_G = \frac{cps_1}{cps_2} \frac{k_{c,1}}{k_{c,2} k_{d,2}} \tag{8}$$

Finally, the HPGe detector efficiency for the different foils at contact can be determined:

$$\epsilon_c = \epsilon_{10} \cdot F_G \tag{9}$$

Being ϵ_c the efficiency at contact, ϵ_{10} the efficiency at 10 cm (obtained by the fit in 4) and F_G the geometric factor (obtained by equation 8).

4 ACS proof of concept

The Torino e-LiBANS facility was used to test the prototypes of ACS. The epithermal configuration was used, and the results were compared to the BSS measurement produced in [17]. The experimental setup was composed by the ACS prototype placed on the top of a specific holder inside the epithermal cavity. The neutron fluence rate was not sufficient to accumulate enough statistics for the 28 mm configuration that was affected by a major neutron absorption in the extra moderator thickness. Therefore, only the 20 mm results are shown. The experimental conditions consisted in 2000 s of neutron irradiation time, 600 s of waiting time between the end of the irradiation and the start of the HPGe acquisition. The integrated epithermal fluence was in the order of 10^8 cm^{-2} s^{-1}.The acquisition times at the HPGe detector can vary depending on several parameters (gamma energy, half-life, cross sections, etc.). For the Torino measurements, they ranged from 1-2 min for the In and Au foils to 3-4 h for the NaCl and Cu foils. The time was adjusted to achieve a counting uncertainty below 1-2%. A picture of the experimental configuration is shown in Fig. 5.

The elements activities $A(t_{irr}, t_{wait})$ were measured at the HPGe detector, and the saturation activity A_{sat} was calculated using equation 10:

$$A(t_{irr}, t_{wait}) = A_{sat}(1 - e^{-\lambda t_{irr}})e^{-\lambda t_{wait}} \tag{10}$$

The values were then corrected again considering the γ self-absorption processes inside the foils. This phenomenon is almost negligible for high γ energies (e.g. In and Na), but becomes relevant for low γ energies (e.g. Re and W). The final values of the saturation activity are reported in Table 2:

The mass specific activities were calculated. To perform an unfolding procedure, one needs the experimental data (Table 2), a set of response curves (Fig. 3), and a priori information like a guess spectrum, usually extracted by Monte Carlo simulations, for this work, the guess was taken from [17]. For the unfolding, the FRUIT code has been used [18]. The outputs of the process are shown in Fig. 6, and the BSS spectrum was taken from previous work [17].

Some considerations, depending on the energy region, can be done:

Table 2 Activation results for the 20 mm ACS radius configuration with 9 sensitive elements

Element	Activity (Bq)	Mass (g)
^{115}In	$1.05\ (0.02) \cdot 10^4$	0.125(0.001)
^{197}Au	$8.46\ (0.20) \cdot 10^3$	0.246(0.001)
^{55}Mn	$4.31\ (0.13) \cdot 10^2$	0.148(0.001)
^{63}Cu	$5.61\ (0.17) \cdot 10^2$	0.797(0.003)
^{23}Na	$8.69\ (0.57) \cdot 10^1$	0.372(0.002)
^{51}V	$2.63\ (0.14) \cdot 10^2$	0.249(0.002)
^{185}Re	$4.37\ (0.24) \cdot 10^4$	0.980(0.002)
^{187}Re	$2.26\ (0.12) \cdot 10^4$	1.639(0.001)
^{186}W	$5.28\ (0.16) \cdot 10^3$	0.687(0.001)

The irradiation time was around 2000s, corresponding to an integrated epithermal fluence in the order of 10^8 cm^{-2} s^{-1}

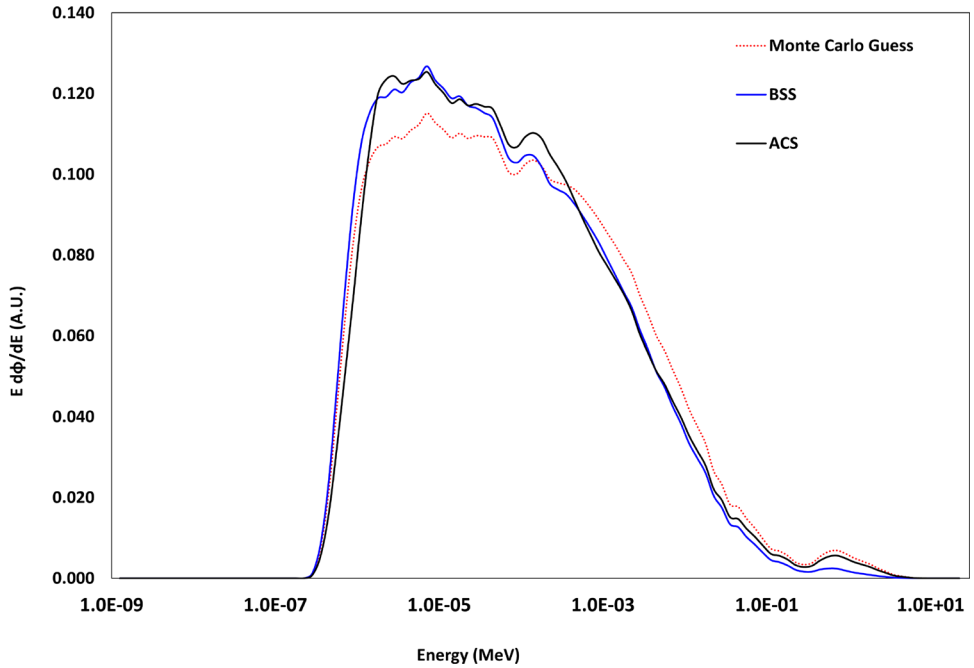

Fig. 6 Comparison between BSS and ACS results. The data have been collected at the e-LiBANS calibrated epithermal neutron source in Torino [17] and have been unfolded using the FRUIT code [18]. In red, the a priori guess spectrum is also shown. The spectra have been normalized to unit area

- Below 0.4 eV, the curves go to zero due to the presence of a Cd shield around the e-LiBANS cavity;
- In the region between 0.4 eV and 100 keV, the BSS and ACS unfolded spectra provide similar results and the agreement is excellent. In particular, the dispersion on the ratio between the two set of data is below 6%;
- Above the 100 keV value, the ACS sensitivity decreases and the unfolding algorithm has no information in the fast peak region at 1 MeV. Therefore, the neutron energy sensitivity for ACS should be limited at 100 keV.

It can be concluded that the comparison between the BSS and the ACS results is excellent over all the epithermal energy range. Nevertheless, some fluctuations in the 1 eV and 800 eV regions are present, here the In and Mn resonances dominate and could alter the shape of the spectrum. The dispersion of the ratio over the range 0.4 eV - 100 keV has been found to be less than 6%.

5 Conclusions

This work conceived and developed a compact epithermal neutron spectrometer, based on the activation neutron phenomenon known as ACS. The device's dimensions are in the order of few cm, and it can be used in a single neutron irradiation, reducing the measuring times. An extensive research and Monte Carlo simulation work has been done to optimize the geometry and composition of ACS. The anisotropy is within 2.5% and the neutron energy sensitivity ranges from thermal up to 100 keV. The first measurements performed at the Torino LINAC facility e-LiBANS revealed an excellent agreement with the standard BSS technique, with a dispersion of less than 6%. Many measurements were produced, revealing a good reproducibility over time.

ACS can measure epithermal spectra in reduced volumes with precision and efficiency comparable to standard techniques. This could represent a significant advancement for beam quality assurance and in-phantom measurements in neutron applications such as BNCT.

Funding Open access funding provided by Università degli Studi di Torino within the CRUI-CARE Agreement. Funding was provided by Dipartimento di Fisica, Università degli Studi di Torino.

Data Availability All the nuclear data used have been taken from public data libraries or publications available at: https://t2.lanl.gov/nis/data/endf/endfvii.1-n.html. https://dx.doi.org/10.1007/bf02518906. https://doi.org/10.1016/S0092-640X(03)00036-6. https://inis.iaea.org/records/mevyg-frk14. https://www.iaea.org/publications/820/practical-aspects-of-operating-a-neutron-activation-analysis-laboratory. https://nucleardata.nuclear.lu.se/toi/perchart.htm. The manuscript has associated data in a data repository.

Declarations

Conflict of interest The corresponding author Ettore Mafucci is listed as the holder of the patent issued under the number 102024000005716

References

1. Advances in Boron Neutron Capture Therapy. Non-serial Publications. INTERNATIONAL ATOMIC ENERGY AGENCY, Vienna (2023). https://www.iaea.org/publications/15339/advances-in-boron-neutron-capture-therapy
2. R.L. Bramblett, R.I. Ewing, T.W. Bonner, A new type of neutron spectrometer. Nuclear Instrum. Methods **9**(1), 1–12 (1960). https://doi.org/10.1016/0029-554X(60)90043-4
3. D.J. Thomas, A.V. Alevra, Bonner sphere spectrometers–a critical review. Nucl. Instrum. Methods Phys. Res. A **476**(1–2), 12–20 (2002)
4. ENDF/B-VII.1 Incident-Neutron Data. https://t2.lanl.gov/nis/data/endf/endfvii.1-n.html
5. E.M. Mafucci, Development of a compact neutron spectrometer for BNCT based on multi-element activation analysis. https://www.researchgate.net/publication/388416140_Development_of_a_compact_neutron_spectrometer_for_BNCT_based_on_multi-element_activation_analysis (2024)
6. E. Mafucci, M. Costa, E. Durisi, V. Monti, R. Bedogni, A. Calamida, Development of a compact neutron spectrometer based on multi-element activation. Nucl. Instrum. Methods Phys. Res. A **1069**(169952), 169952 (2024)
7. A. Simonits, L. Moens, F. Corte, A. Wispelaere, A. Elek, J. Hoste, Ko-measurements and related nuclear data compilation for (n, γ) reactor neutron activation analysis. J. Radioanal. Chem. **60**(2), 461–516 (1980)
8. F. De Corte, A. Simonits, Recommended nuclear data for use in the k0 standardization of neutron activation analysis. At. Data Nucl. Data Tables **85**(1), 47–67 (2003)
9. J. Kopecky, J. Sublet, S. C, A. J, R. Forrest, N. A, D: Atlas of neutron capture cross sections (1997)
10. Practical Aspects of Operating A Neutron Activation Analysis Laboratory. TECDOC Series, vol. 564. International ATomic Energy Agency, Vienna (1990). https://www.iaea.org/publications/820/practical-aspects-of-operating-a-neutron-activation-analysis-laboratory
11. Database WWW Table of Radioactive Isotopes. https://nucleardata.nuclear.lu.se/toi/perchart.htm
12. S. Mughabghab, Atlas of Neutron Resonances: Resonance Parameters and Thermal Cross Sections Z= 1-100, (2006)
13. T.B. Ryves, A new thermal neutron flux convention. Metrologia **5**(4), 119–124 (1969)
14. N.P. Baumann, Resonance Integrals and Self-shielding Factors for Detecor Foils (1963)
15. ORTEC data sheet. https://www.ortec-online.com/-/media/ametekortec/brochures/g/gem-a4.pdf?la=en&revision=127d8898-b91f-4052-b632-038e5247564d
16. K. Debertin, R.G. Helmer, *Gamma- and X-ray Spectrometry with Semiconductor Detectors* (North-Holland, Netherlands, 1988)
17. V. Monti, M. Costa, E. Durisi, M. Ferrero, L. Menzio, O. Sans-Planell, L. Visca, R. Bedogni, M. Treccani, K. Alikaniotis, G. Giannini, The E LiBANS project: Thermal and epithermal neutron sources based on a medical linac. Appl. Radiat. Isot. **166**(109363), 109363 (2020)
18. R. Bedogni, C. Domingo, A. Esposito, F. Fernández, FRUIT: An operational tool for multisphere neutron spectrometry in workplaces. Nucl. Instrum. Methods Phys. Res. A **580**(3), 1301–1309 (2007)